



OPEN

Prediction of properties of boron α -icosahedral nanosheet by bond-addictive M -polynomial

D. Antony Xavier¹, K. Julietraja², Ammar Alsinai^{3,4✉} & S. Akhila¹

Nanosheets with boron elements have excellent characteristics which makes the boron polymorphs unique and super hard. A boron α -icosahedral nanosheet in crystalline form has superconductivity and thermal electronic properties. In theoretical chemistry and QSPR/QSAR study, a topological descriptor is an important analytical tool. It helps to analyse the structure and its properties and also correlates the with numerical expressions. The valence-based M -polynomial provides quantitative measures of molecular properties based on their geometric, electrostatic, and quantum chemical characteristics. In this article, the QSPR/QSAR analysis is performed for this nanosheet and the analytical expressions are validated with original synthesized data, and received excellent correlation values of 0.9835 and 0.9932. The mathematical expression of the structure is analysed and the indices are compared graphically and numerically.

Boron is an interesting and complex element, many aspects of which are still to be explored. The properties of boron are found between metals and insulators. While boron has only three valence electrons, which would favor metallicity, they are localized enough to produce insulating states. However, pressure, temperature, and impurities can easily shift this subtle balance between metallic and insulating states. Pure boron is one of the best alternatives to carbon fullerenes (CFs) and nanotubes (CNTs), which exhibit superior properties, in the form of novel solids and nanostructures, such as quasiplanar clusters, quasi-crystals, nanosheets, nanoribbons, nano chains, and nanotubes¹. Besides being the only non-metal element in Group III, boron is unique in its structural complexity and has exceptional chemical and physical properties, including low densities, high melting points, and high hardness². Initially, Boron exists in three crystalline forms, $\alpha - B_{12}$, $\beta - B_{106}$ and $\gamma - B_{28}$ ³. Later different forms of boron crystalline have been synthesized, such as α - rhombohedral, β -rhombohedral, tetragonal, γ -orthorhombic, and α -Ga type. In addition, there are amorphous phases and nanosized structures⁴. One of them is the B_{12} icosahedral that is linked together by “inter-icosahedral covalent units” or “chains”⁵. The boron-rich ceramics based on icosahedral are second only to diamonds as hard materials. When compared to diamond-based materials, this class of ceramics offer low density, better thermal and chemical resistance, and ease of mass production.

In boron α -icosahedral nanosheet, each crystal contains an icosahedron molecule of B_{12} , which is linked to form a three-dimensional network¹ as shown in Fig. 1. A regular icosahedron has 12 vertices, 30 edges and 20 faces. The icosahedral boron sheet, B_{12} and B_{20} have been proposed in recent years with special properties. Kah et al.⁶ proposed many icosahedral nanosheets based on B_{12} clusters, and Zhou et al.⁷ presented an antiferromagnetic metallic B_{20} sheet. Higashi et al.⁸ investigated the first 2D icosahedral B_{12} networks. The icosahedral nanosheet bonding is complex and was well explained by Emin⁹. The boron allotropes attract major material researchers since they exhibit properties like thermal conductivity, hardness, and neutron scattering length¹⁰. The novel icosahedral structures exhibit interesting chemical bonding and electronic properties and are structurally and energetically stable. Additionally, these α -icosahedral nanosheets, which are a gapless system, exhibit semiconducting properties, suggesting an application in nanoelectronics and computer chips. is a good choice, In industrial semiconductor applications like solar cells with high solar light conversion efficiency, the icosahedral boron nanosheet is a prominent component¹¹.

In a molecular graph, each edge of a molecule corresponds to a chemical bond between atoms, while each vertex and degree denotes an atom and valence of the atom. In order to characterize the structural features of these molecules, several theoretical tools are employed. A topological index can be used to model relationships between chemical structures and their corresponding biochemical and physicochemical activities^{12,13}. Large

¹Department of Mathematics, Loyola College (Affiliated to the University of Madras), Chennai, India. ²Department of Mathematics, School of Engineering, Presidency University, Bengaluru 560064, India. ³Department of Mathematics, Ibb university, Ibb, Yemen. ⁴Department of Mathematics, Kuvempu University, Shivamogga, Karnataka 577451, India. ✉email: aliiammara1985@gmail.com

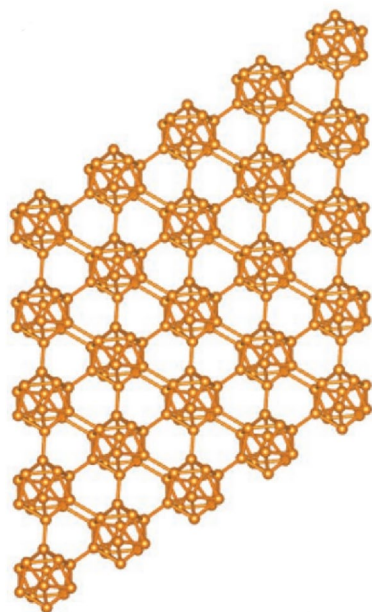


Figure 1. Crystal structure of boron α -icosahedral nanosheet.

combinatorial chemical libraries are required to compute the physicochemical properties of a structure. These include novel development methods such as topological structural descriptors, combinatorial quantum chemistry tools for functional group analysis, shape-activity relations, and topological attributes of electron densities, etc. The degree-based topological indexes are used extensively in network science for investigating networks, in which the indexes are calculated based on the degrees of the graph. A breakthrough was made in degree-based indices by Deutsch and Klavžar¹⁴, introducing the M-polynomial. Readers can refer to^{15–18} for recent work in M-polynomial and topological indices.

Boron α -icosahedral nanosheets are grabbing immense attention due to their numerous applications in emerging technologies. Thus, understanding the properties of these structures is imperative for industrial applications. In this paper, the degree-based structure analysis of α -icosahedral nanosheet is performed using M-polynomial. The analytical expressions for some prominent indices are evaluated and their graphical representations are plotted using the numerical values of these indices and compared. The shear modulus and Young's modulus of the icosahedral nanosheet are compared against its structural parameters, which helps to predict the properties of numerous additional boron allotropes.

Computational techniques

A chemical compound can be modeled as a simple graph, χ with vertex and edge sets, $\mathcal{V}(\chi)$ and $\mathcal{E}(\chi)$ respectively. The valency of an atom is denoted by d_μ of the vertex $\mu \in \mathcal{V}(\chi)$, whereas the maximum degree over all the vertices of χ is denoted by Ψ . The degree of the vertex of boron α -icosahedral nanosheet is illustrated in Fig. 2. The set are consider, $\mathfrak{D} = \{(\ell, h) \in \mathbb{N} \times \mathbb{N} | 1 \leq \ell \leq h \leq \Psi\}$. We denote $d_{\ell, h} = |\{\mu\eta \in \mathcal{E}(\chi) | d_\mu = \ell \text{ and } d_\eta = h\}|$. The M-polynomial¹⁴ for simple connected graph, χ is defined by

$$M(\chi; \eta, z) = \sum_{\ell \leq h} m_{\ell, h}(\chi) \eta^\ell z^h \quad (1)$$

where $m_{\ell, h}(\chi)$ be the total number of edges $\mu\eta \in \mathcal{E}(\chi)$ such that $\{d_\mu, d_\eta\} = \{\ell, h\}$. The bond additive is the function from χ into \mathbb{R} specified as real numbers $\beta_{\ell, h}$, $(\ell, h) \in \mathfrak{D}$ induced by $\beta(\chi) = \sum_{(\ell, h) \in \mathfrak{D}} d_{\ell, h} \beta_{\ell, h}$. The degree-based structural descriptors for χ , where $\mathfrak{f}(d_\mu, d_\eta)$ is the function of degree based indices is depicted as

$$\Lambda(\chi) = \sum_{\mu\eta \in \mathfrak{D}} \mathfrak{f}(d_\mu, d_\eta)$$

A brief discussion of bond additive degree-based indices is given below regarding the above-specified real numbers, $\beta_{\ell, h}$. First degree-based structure descriptors were studied¹⁹ and developed²⁰ with the Zagreb index, $M_1(\chi)$ defined by $\beta_{\ell, h} = \ell + h$ based on the square root of the vertex degrees to analyze the influence of total electron energy on structure. The next analogous of Zagreb index is *second Zagreb index*, $M_2(\chi)$ represented as $\beta_{\ell, h} = \ell h$. These indices help in analyzing the complexity of the molecular system and increase with extent branching of the carbon skeleton. The other analogous of Zagreb index are *augmented Zagreb index*, $AZ(\chi)$ ²¹ and *hyper Zagreb index*, $HM(\chi)$ ²² is defined by $\beta_{\ell, h} = \left(\frac{\ell h}{\ell + h - 2}\right)^3$ and $\beta_{\ell, h} = (\ell + h)^2$ respectively. These indices

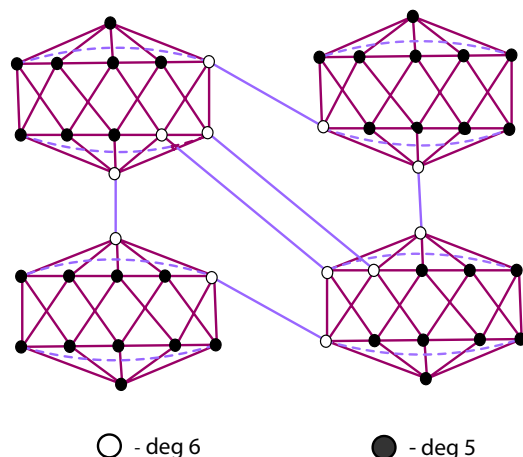


Figure 2. Degree of boron α -icosahedral nanosheet.

are used to analyze new drugs' molecular structures and to understand their biological and chemical properties. Based on the inverse value of vertex degree, the other invariant of Zagreb index, *modified Zagreb*, $M_2^m(\chi)$ ²³ defined by $\beta_{\ell h} = \frac{1}{\ell h}$ is evolved. Several studies have demonstrated that the augmented Zagreb index can predict the temperature at which octanes and heptanes form. These variants of Zagreb indices can be used for determining the isomerism of ZE, chirality, heat formation, and heterogeneity of hetero systems.

Based on the degrees of the end vertices of χ , several methods have been proposed to examine the branching properties of alkanes. In 1975 Milan Randić²⁴ developed the topological index of graph, χ under the label "molecular connectivity index" in the description R_{-1} and $R_{-1/2}$. A *general Randić index*, $R_{\vartheta}(\chi)$ latterly developed by Bollobas and Erdos²⁵ by substituting R_{-1} and $R_{-1/2}$ with a real integer ϑ is defined as $\beta_{\ell h} = (\ell h)^{\vartheta}$. The other variant of randić index are *reciprocal randić*, $RR_{\vartheta}(\chi)$ ²⁶ and *harmonic index*, $H(\chi)$ ²⁷ are represented as $\beta_{\ell h} = \frac{1}{(\ell h)^{\vartheta}}$ and $\beta_{\ell h} = \frac{2}{\ell + h}$. Graph eigenvalues were analyzed by Favaron et al.²⁸ in relation to harmonic indices. A correlation has been demonstrated between these variants of randić index and various physicochemical properties of alkanes, including the formation of enthalpies, surface areas, vapor pressure, boiling points, Kovats constants, and so on²⁹.

Symmetric division degree index, $SSD(\chi)$ ³⁰ is a great tool for predicting polychlorobiphenyl surfaces is defined by $\beta_{\ell h} = \frac{\ell}{h} + \frac{h}{\ell}$ or $\beta_{\ell h} = \frac{\ell^2 + h^2}{\ell h}$. *Forgotten index*, $F(\chi)$ ³¹, which greatly enhances the physicochemical prediction of the First Zagreb index, and it is defined as $\beta_{\ell h} = \ell^2 + h^2$. An important tool for estimating octane isomer surface area is the *inverse sum index* $I(\chi)$ ³² defined as $\beta_{\ell h} = \frac{\ell h}{\ell + h}$. And *sigma index*, $\sigma(\chi)$ is given by $\beta_{\ell h} = (\ell - h)^2$. By analyzing the above discussion, it is evident that the bond additive degree is a significant aspect to investigate the physicochemical properties of molecular structures. Table 1 outlines the formulations for the M-polynomial method.

The operators are required which relate the degree-based topological descriptors with the \mathbb{M} -polynomial,

Topological indices	$\mathbb{f}(\eta, \delta)$	Derivation from $\mathbb{M}(\chi)$
$M_1(\chi)$	$\eta + \delta$	$(D_{\eta} + D_{\delta})(\mathbb{M}(\chi); \eta, \delta) _{\eta=\delta=1}$
$M_2(\chi)$	$\eta\delta$	$(D_{\eta}D_{\delta})(\mathbb{M}(\chi); \eta, \delta) _{\eta=\delta=1}$
$M_2^m(\chi)$	$\frac{1}{\eta\delta}$	$(S_{\eta}S_{\delta})(\mathbb{M}(\chi); \eta, \delta) _{\eta=\delta=1}$
$A(\chi)$	$(\frac{\eta\delta}{\eta+\delta-2})^3$	$(S_{\eta}^3Q_{-2}D_{\eta}^3D_{\delta}^3)(\mathbb{M}(\chi); \eta, \delta) _{\eta=\delta=1}$
$R_{\vartheta}(\chi)$	$(\eta\delta)^{\vartheta}$	$(D_{\eta}^{\vartheta} + D_{\delta}^{\vartheta})(\mathbb{M}(\chi); \eta, \delta) _{\eta=\delta=1}$
$RR_{\vartheta}(\chi)$	$(\frac{1}{\eta\delta})^{\vartheta}$	$S_{\eta}^{\vartheta}S_{\delta}^{\vartheta}(D_{\eta} + D_{\delta})(\mathbb{M}(\chi); \eta, \delta) _{\eta=\delta=1}$
$H(\chi)$	$\frac{2}{\eta+\delta}$	$2S_{\eta}J(\mathbb{M}(\chi); \eta, \delta) _{\eta=\delta=1}$
$HM(\chi)$	$(\eta + \delta)^2$	$(D_{\eta} + D_{\delta})^2(\mathbb{M}(\chi); \eta, \delta) _{\eta=\delta=1}$
$F(\chi)$	$\eta^2 + \delta^2$	$(D_{\eta}^2 + D_{\delta}^2)(\mathbb{M}(\chi); \eta, \delta) _{\eta=\delta=1}$
$\sigma(\chi)$	$(\eta - \delta)^2$	$(D_{\eta} - D_{\delta})^2(\mathbb{M}(\chi); \eta, \delta) _{\eta=\delta=1}$
$SDD(\chi)$	$\frac{\eta^2 + \delta^2}{\eta\delta}$	$(D_{\eta}S_{\delta} + D_{\delta}S_{\eta})(\mathbb{M}(\chi); \eta, \delta) _{\eta=\delta=1}$
$I(\chi)$	$\frac{\eta\delta}{\eta+\delta}$	$(S_{\eta}JD_{\eta}D_{\delta})(\mathbb{M}(\chi); \eta, \delta) _{\eta=1}$

Table 1. The derivation of vertex-degree \mathbb{M} -polynomials.

$$D_\eta(\xi(\eta, \zeta)) = \eta \frac{\partial(\xi(\eta, \zeta))}{\partial \eta}, D_\zeta(\xi(\eta, \zeta)) = \zeta \frac{\partial(\xi(\eta, \zeta))}{\partial \zeta}, S_\eta(\xi(\eta, \zeta)) = \int_0^\eta \frac{\xi(q, \zeta)}{q} dq$$

$$S_\zeta(\xi(\eta, \zeta)) = \int_0^\zeta \frac{\xi(\eta, q)}{q} dq, J(\xi(\eta, \zeta)) = \xi(\eta, \eta), Q_\kappa(\xi(\eta, \zeta)) = \eta^\kappa \xi(\eta, \zeta); \kappa \neq 0.$$

Main results and discussion
M-polynomial of boron α -icosahedral nanosheet

Theorem 1 If $\chi = I_\alpha(s, p)|s, p \geq 1$ represents a boron α -icosahedral nanosheet, then M-polynomial is

$$\mathbb{M}(I_\alpha(s, p); \eta, \zeta) = (4sp + 14s + 16p - 4)\eta^5\zeta^5 + (12sp - 2p + 2s - 12)\eta^5\zeta^6 + (18sp - 17p - 19s + 18)\eta^6\zeta^6$$

Proof The boron α -icosahedral nanosheet, $I_\alpha(s, p)|s, p \geq 1$ contains $12sp$ vertices and $34sp - 3s - 3p + 2$ edges. icosahedral nanosheets are categorized into edge sets based on the degree of the vertex, $\mathcal{D} = \{(5, 5), (5, 6), (6, 6)\}$. The edge partition of $I_\alpha(s, p)$ based on the vertex degree is depicted in Fig. 3. The edge sets, $\mathcal{E}(I_\alpha(s, p))$ is classified into three types and the parameter value, $d_{\eta\zeta}$ is characterized by the following value,

$$d_{55} = |\{\mu\eta \in \mathcal{E}(I_\alpha(s, p)) | d_\mu = 5 \text{ and } d_\eta = 5\}| = 4sp + 14s + 16p - 4$$

$$d_{56} = |\{\mu\eta \in \mathcal{E}(I_\alpha(s, p)) | d_\mu = 5 \text{ and } d_\eta = 6\}| = 12sp + 2s - 2p - 12$$

$$d_{66} = |\{\mu\eta \in \mathcal{E}(I_\alpha(s, p)) | d_\mu = 6 \text{ and } d_\eta = 6\}| = 18sp - 19s - 17p + 18$$

By the Definition (1), M-polynomial of boron α -icosahedral nanosheet, $I_\alpha(s, p)|s, p \geq 1$ is defined as

$$\mathbb{M}(I_\alpha(s, p); \eta, \zeta) = \sum_{\xi \leq \eta} m_{\xi\eta}(I_\alpha(s, p))\eta^\xi\zeta^\eta$$

Figure 4 shows the graphical illustration of the M-polynomial function of $I_\alpha(s, p)|s = 4$ and $p = 5$. Thus, $\mathbb{M}(I_\alpha(s, p); \eta, \zeta)$ can be formulated as,

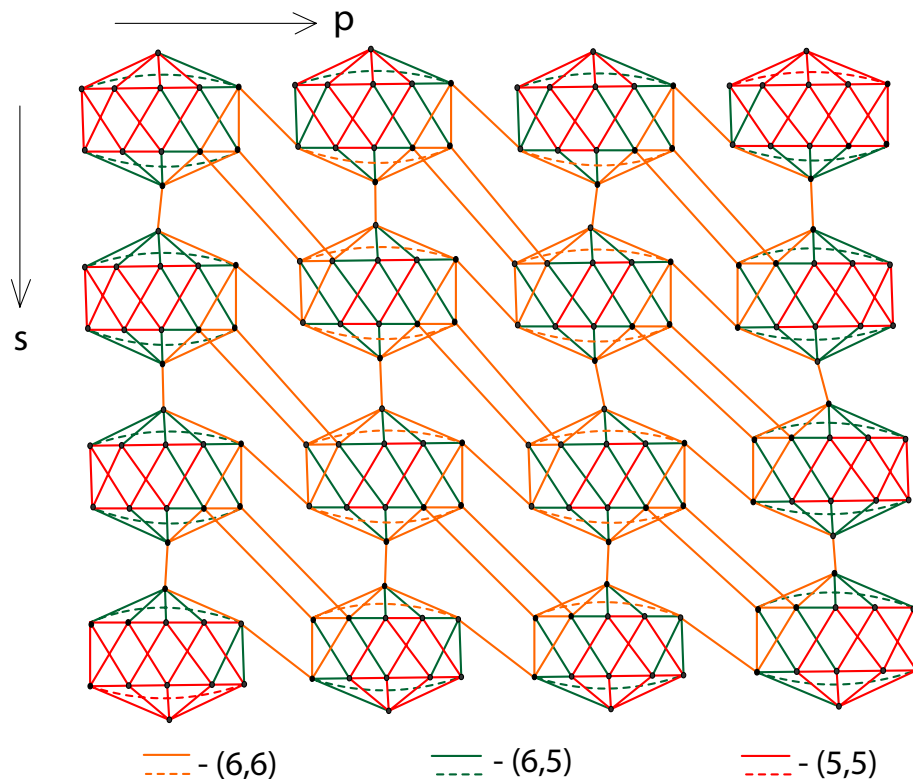


Figure 3. Edge partition of boron α -icosahedral nanosheet, $I_\alpha(4, 4)$.

$$\begin{aligned} \mathbb{M}(I_\alpha(s, p); \eta, \zeta) &= \sum_{5 \leq 5} m_{55}(I_\alpha(s, p))\eta^5 \zeta^5 + \sum_{5 \leq 6} m_{56}(I_\alpha(s, p))\eta^5 \zeta^6 + \sum_{6 \leq 6} m_{66}(I_\alpha(s, p))\eta^6 \zeta^6 \\ &= d_{55}\eta^5 \zeta^5 + d_{56}\eta^5 \zeta^6 + d_{66}\eta^6 \zeta^6 \\ &= (4sp + 14s + 16p - 4)\eta^5 \zeta^5 + (12sp - 2p + 2s - 12)\eta^5 \zeta^6 \\ &\quad + (18sp - 17p - 19s + 18)\eta^6 \zeta^6 \end{aligned}$$

Results for boron α -icosahedral nanosheet

Using Theorem 1 and \mathbb{M} -polynomial formula in Table 1, vertex degree-based topological indices such as $M_1, M_2, M_2^m, A, R_D, RR_D, H, HM, F, \sigma, SDD$ and I of boron α -icosahedral nanosheet, $I_\alpha(s, p) | s, p \geq 1$ are computed. Here, $f(\eta, \zeta) = \mathbb{M}(I_\alpha(s, p); \eta, \zeta) = (4sp + 14s + 16p - 4)\eta^5 \zeta^5 + (12sp - 2p + 2s - 12)\eta^5 \zeta^6 + (18sp - 17p - 19s + 18)\eta^6 \zeta^6$. The numerical value of the derived analytical expression is compared with each index is depicted in Tables 2, 3, 4 and 5. And the graphical comparison is illustrated in Figs. 5, 6 and 7.

Theorem 2 Let $I_\alpha(s, p) | s, p \geq 1$ be a boron α -icosahedral nanosheet then

1. $M_1(I_\alpha(s, p)) = 388sp - 66p - 66s + 44$
2. $R_D(I_\alpha(s, p)) = 1108sp - 272p - 274s + 188$
3. $I(I_\alpha(s, p)) = \frac{1064sp}{89s} - \frac{181p}{91p} - \frac{182s}{53sp} + \frac{124}{50}$
4. $RR_D(I_\alpha(s, p)) = \frac{11}{900} + \frac{11}{900} + \frac{53sp}{50} - \frac{3}{50}$

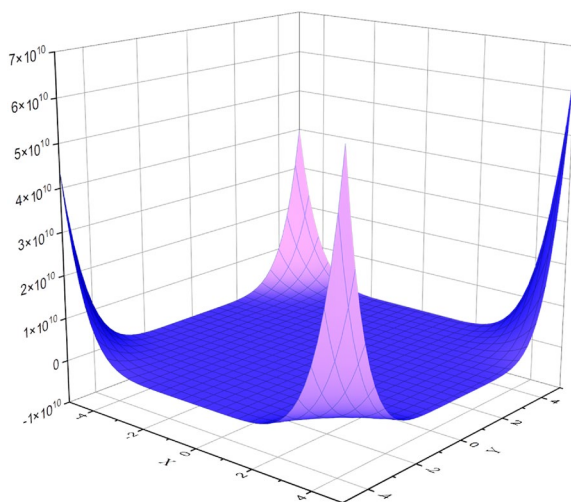


Figure 4. \mathbb{M} -polynomial of boron α -icosahedral nanosheet, $I_\alpha(4, 5)$.

(s, p)	$M_1(I_\alpha(s, p))$	$R_D(I_\alpha(s, p))$	$I(I_\alpha(s, p))$	$RR_D(I_\alpha(s, p))$
(1, 1)	300	750	75	1.2
(1, 2)	622	1586	155.2727	2.3611
(2, 2)	1332	3528	332.1818	4.58
(3, 3)	3140	8522	782.8182	10.08
(4, 3)	4238	11572	1056.4545	13.3589
(5, 5)	9084	25158	2264.4545	27.44
(5, 6)	10958	30426	2731.6364	32.8411
(6, 6)	13220	36800	3295.4545	39.3
(6, 7)	15482	43176	3859.3636	45.7611
(7, 8)	20782	58142	5180.5454	60.8011

Table 2. Numerical value of $M_1(I_\alpha(s, p)) R_D(I_\alpha(s, p)) I(I_\alpha(s, p)) RR_D(I_\alpha(s, p))$.

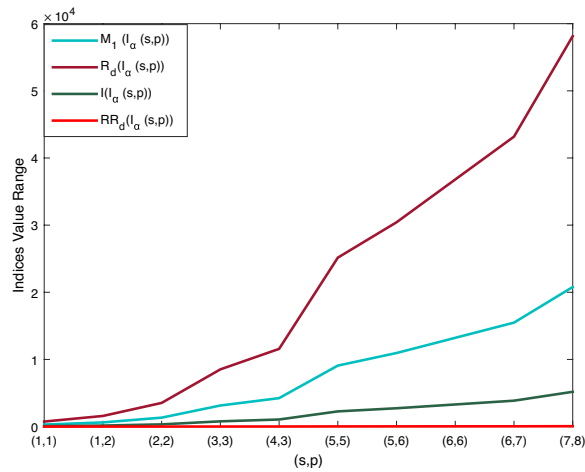


Figure 5. Visualization of $M_1(I_\alpha(s, p))$, $R_\Delta(I_\alpha(s, p))$, $I(I_\alpha(s, p))$, $RR_\Delta(I_\alpha(s, p))$.

(s, p)	$M_2(I_\alpha(s, p))$	$F(I_\alpha(s, p))$	$A(I_\alpha(s, p))$	$HM(I_\alpha(s, p))$
(1, 1)	750	1500	915.5273	3000
(1, 2)	1586	3182	1942.9053	6354
(2, 2)	3528	7092	4370.407	14148
(3, 3)	8522	17140	10637.9321	34184
(4, 3)	11572	23278	14471.7565	46422
(5, 5)	25158	50604	31610.9189	100920
(5, 6)	30426	61198	38263.5878	122050
(6, 6)	36800	74020	46316.3806	147620
(6, 7)	43176	86842	54375.3723	173194
(7, 8)	58142	116942	73299.8022	233226

Table 3. Numerical value of $M_2(I_\alpha(s, p))$ $F(I_\alpha(s, p))$ $A(I_\alpha(s, p))$ $HM(I_\alpha(s, p))$.

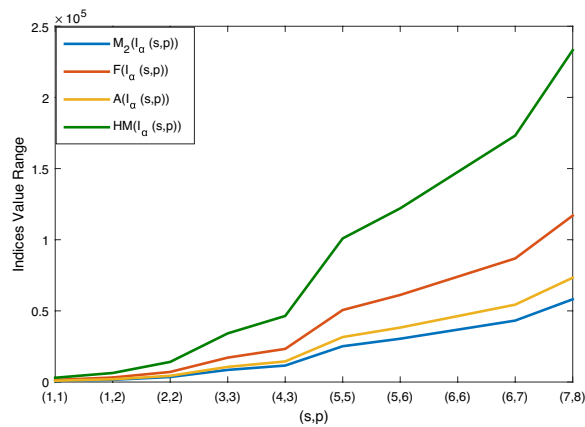


Figure 6. Graphical representation of $M_2(I_\alpha(s, p))$ $F(I_\alpha(s, p))$ $A(I_\alpha(s, p))$ $HM(I_\alpha(s, p))$.

Proof

$$1. M_1(I_\alpha(s, p)) = (D_\eta + D_\zeta)(\mathbb{M}(I_\alpha(s, p)); \eta, \zeta)|_{\eta=\zeta=1}$$

(s, p)	$M_2^m(I_\alpha(s, p))$	$SDD(I_\alpha(s, p))$	$H(I_\alpha(s, p))$	$\sigma(I_\alpha(s, p))$
(1, 1)	1.2	60	6	0
(1, 2)	2.3611	122.3333	11.9848	10
(2, 2)	4.58	253.2	23.9455	36
(3, 3)	10.08	583.2	53.8545	96
(4, 3)	13.3589	782.4667	71.797	134
(5, 5)	27.44	1653.6	149.5636	288
(5, 6)	32.8411	1989.5333	179.4758	346
(6, 6)	39.3	2394	215.3637	420
(6, 7)	45.7611	2798.3333	251.2576	490
(7, 8)	60.8011	3743.9333	335.003	658

Table 4. Numerical value of $M_2^m(I_\alpha(s, p)), SDD(I_\alpha(s, p)), H(I_\alpha(s, p)), \sigma(I_\alpha(s, p))$.

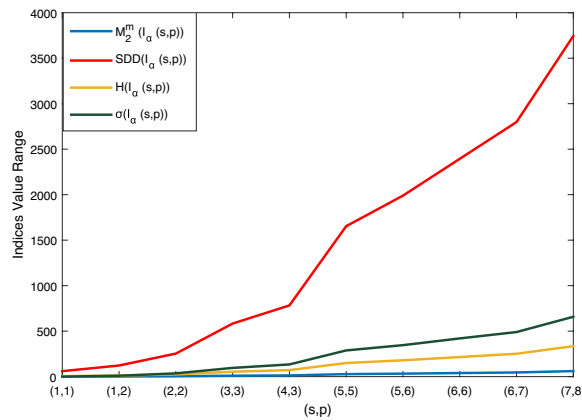


Figure 7. Graphical illustration of $M_2^m(I_\alpha(s, p)), SDD(I_\alpha(s, p)), H(I_\alpha(s, p)), \sigma(I_\alpha(s, p))$.

$$\begin{aligned}
 (D_\eta + D_3)(\mathfrak{f}(\eta, \mathfrak{z})) &= 2\eta^5 \mathfrak{z}^5 (70s + 80p - 66\mathfrak{z} + 20s\mathfrak{p} + 11s\mathfrak{z} - 11p\mathfrak{z} + 108\eta\mathfrak{z} + 66s\mathfrak{p}\mathfrak{z} \\
 &\quad - 114s\eta\mathfrak{z} - 102p\eta\mathfrak{z} + 108s\mathfrak{p}\eta\mathfrak{z} - 20) \Big|_{\eta=\mathfrak{z}=1} \\
 &= 388s\mathfrak{p} - 66p - 66s + 44
 \end{aligned}$$

$$2. \quad R_\mathfrak{d}(I_\alpha(s, p)) = (D_\eta^\mathfrak{d} + D_3^\mathfrak{d})(\mathbb{M}(I_\alpha(s, p)); \eta, \mathfrak{z}) \Big|_{\eta=\mathfrak{z}=1}$$

$$\begin{aligned}
 (D_\eta^\mathfrak{d} + D_3^\mathfrak{d})(\mathfrak{f}(\eta, \mathfrak{z})) &= 5^{2\mathfrak{d}} (14s + 16p + 4s\mathfrak{p} - 4) - 6^{2\mathfrak{d}} (19s + 17p - 18s\mathfrak{p} - 18) \\
 &\quad + 5^\mathfrak{d} 6^\mathfrak{d} (2s - 2p + 12s\mathfrak{p} - 12) \Big|_{\eta=\mathfrak{z}=1; \mathfrak{d}=1} \\
 &= 1108s\mathfrak{p} - 272p - 274s + 188
 \end{aligned}$$

$$3. \quad I(I_\alpha(s, p)) = (S_\eta J D_\eta D_3)(\mathbb{M}(I_\alpha(s, p)); \eta, \mathfrak{z})$$

$$\begin{aligned}
 (S_\eta J D_\eta D_3)(\mathfrak{f}(\eta, \mathfrak{z})) &= \eta^{12} (54s\mathfrak{p} - 51p - 57s + 54) + \eta^{11} \left(\frac{60s}{11} - \frac{60p}{11} \right. \\
 &\quad \left. + \frac{360s\mathfrak{p}}{11} - \frac{360}{11} \right) + \eta^{10} (10s\mathfrak{p} + 35s + 40p - 10) \Big|_{\eta=1} \\
 &= \frac{1064s\mathfrak{p}}{11} - \frac{181p}{11} - \frac{182s}{11} + \frac{124}{11}
 \end{aligned}$$

$$4. \quad RR_\mathfrak{d}(I_\alpha(s, p)) = S_\eta^\mathfrak{d} S_3^\mathfrak{d} (D_\eta + D_3)(\mathbb{M}(I_\alpha(s, p)); \eta, \mathfrak{z})$$

$$\begin{aligned}
 S_{\eta}^{\delta} S_{\zeta}^{\delta}(\mathfrak{f}(\eta, \zeta)) &= \frac{1}{52\delta} (14s + 16p + 4sp - 4) + \frac{1}{30\delta} (2s - 2p + 12sp - 12) \\
 &\quad - \frac{1}{62\delta} (19s + 17p - 18sp - 18) \Big|_{\eta=\zeta=1; \delta=1} \\
 &= \frac{89s}{900} + \frac{91p}{900} + \frac{53sp}{50} - \frac{3}{50}
 \end{aligned}$$

Theorem 3 Let $I_{\alpha}(s, p)|_{s, p \geq 1}$ be a boron α -icosahedral nanosheet then

1. $M_2(I_{\alpha}(s, p)) = 1108sp - 272p - 274s + 188$
2. $F(I_{\alpha}(s, p)) = 2228sp - 546p - 546s + 364$
3. $A(I_{\alpha}(s, p)) = \frac{202510477sp}{144000} - \frac{40926041p}{108000} - \frac{332764271s}{864000} + \frac{39354227}{144000}$
4. $HM(I_{\alpha}(s, p)) = 4444sp - 1090p - 1094s + 740$

Proof

1. $M_2(I_{\alpha}(s, p)) = D_{\eta}D_{\zeta}(\mathbb{M}(I_{\alpha}(s, p)); \eta, \zeta)$
 $D_{\eta}D_{\zeta}(\mathfrak{f}(\eta, \zeta)) = \eta\zeta(30\eta^4\zeta^5(2s - 2p + 12sp - 12) + 25\eta^4\zeta^4(14s + 16p + 4sp - 4) - 36\eta^5\zeta^5(19s + 17p - 18sp - 18)) \Big|_{\eta=\zeta=1}$
 $= 1108sp - 272p - 274s + 188$
2. $F(I_{\alpha}(s, p)) = (D_{\eta}^2 + D_{\zeta}^2)(\mathbb{M}(I_{\alpha}(s, p)); \eta, \zeta)$
 $(D_{\eta}^2 + D_{\zeta}^2)(\mathfrak{f}(\eta, \zeta)) = 2\eta^5\zeta^5(350s + 400p - 366\zeta + 100sp + 61s\zeta - 61p\zeta + 648\eta\zeta + 366sp\zeta - 684s\eta\zeta - 612p\eta\zeta + 648ps\eta\zeta - 100) \Big|_{\eta=\zeta=1}$
 $= 2228sp - 546p - 546s + 364$
3. $A(I_{\alpha}(s, p)) = (S_{\eta}^3 Q_{-2} D_{\eta}^3 D_{\zeta}^3)(\mathbb{M}(I_{\alpha}(s, p)); \eta, \zeta)$
 $(S_{\eta}^3 Q_{-2} D_{\eta}^3 D_{\zeta}^3)(\mathfrak{f}(\eta, \zeta)) = \eta^{10} \left(\frac{104976sp}{125} - \frac{99144p}{125} - \frac{110808s}{125} + \frac{104976}{125} \right) + \eta^9 \left(\frac{2000s}{27} - \frac{2000p}{27} + \frac{4000sp}{9} - \frac{4000}{9} \right) + \eta^8 \left(\frac{109375s}{256} + \frac{15625p}{32} + \frac{15625sp}{128} - \frac{15625}{128} \right) \Big|_{\eta=1}$
 $= \frac{202510477sp}{144000} - \frac{40926041p}{108000} - \frac{332764271s}{864000} + \frac{39354227}{144000}$
4. $HM(I_{\alpha}(s, p)) = (D_{\eta} + D_{\zeta})^2(\mathbb{M}(I_{\alpha}(s, p)); \eta, \zeta)$
 $(D_{\eta} + D_{\zeta})^2(\mathfrak{f}(\eta, \zeta)) = 2\eta^5\zeta^5(700s + 800p - 726\zeta + 200sp + 121s\zeta - 121p\zeta + 1296\eta\zeta + 726sp\zeta - 1368s\eta\zeta - 1224p\eta\zeta + 1296sp\eta\zeta - 200) \Big|_{\eta=\zeta=1}$
 $= 4444sp - 1090p - 1094s + 740$

Theorem 4 Let $I_{\alpha}(s, p)|_{s, p \geq 1}$ be a boron α -icosahedral nanosheet then

1. $M_2^m(I_{\alpha}(s, p)) = \frac{89s}{900} + \frac{91p}{900} + \frac{53sp}{50} - \frac{3}{50}$
2. $SDD(I_{\alpha}(s, p)) = \frac{342sp}{5} - \frac{91p}{15} - \frac{89s}{15} + \frac{18}{5}$
3. $H(I_{\alpha}(s, p)) = \frac{p}{330} - \frac{s}{330} + \frac{329sp}{55} + \frac{1}{55}$

$$4. \sigma(I_\alpha(s, p)) = 2s - 2p + 12sp - 12$$

Proof

$$1. M_2^m(I_\alpha(s, p)) = S_\eta S_3(\mathbb{M}(I_\alpha(s, p)); \eta, \zeta)$$

$$\begin{aligned} S_\eta S_3(\mathbb{F}(\eta, \zeta)) &= \frac{\eta^5 \zeta^6 (2s - 2p + 12sp - 12)}{30} + \frac{\eta^5 \zeta^5 (14s + 16p + 4sp - 4)}{25} \\ &\quad - \frac{\eta^6 \zeta^6 (19s + 17p - 18sp - 18)}{36} \Big|_{\eta=\zeta=1} \\ &= \frac{89s}{900} + \frac{91p}{900} + \frac{53sp}{50} - \frac{3}{50} \end{aligned}$$

$$2. SDD(I_\alpha(s, p)) = (D_\eta S_3 + D_\zeta S_\eta)(\mathbb{M}(I_\alpha(s, p)); \eta, \zeta)$$

$$\begin{aligned} (D_\eta S_3 + D_\zeta S_\eta)(\mathbb{F}(\eta, \zeta)) &= \frac{\eta^5 \zeta^5}{15} (420s + 480p - 366\zeta + 120sp + 61s\zeta - 61p\zeta + 540\eta\zeta \\ &\quad + 366sp\zeta - 570s\eta\zeta - 510p\eta\zeta + 540sp\eta\zeta - 120) \Big|_{\eta=\zeta=1} \\ &= \frac{342sp}{5} - \frac{91p}{15} - \frac{89s}{15} + \frac{18}{5} \end{aligned}$$

$$3. H(I_\alpha(s, p)) = 2S_\eta J(\mathbb{M}(I_\alpha(s, p)); \eta, \zeta)$$

$$\begin{aligned} 2S_\eta J(\mathbb{F}(\eta, \zeta)) &= 2\eta^{10} \left(\frac{7s}{5} + \frac{8p}{5} + \frac{2sp}{5} - \frac{2}{5} \right) - 2\eta^{12} \left(\frac{19s}{12} + \frac{17p}{12} - \frac{3sp}{2} - \frac{3}{2} \right) \\ &\quad + 2\eta^{11} \left(\frac{2s}{11} - \frac{2p}{11} + \frac{12sp}{11} - \frac{12}{11} \right) \Big|_{\eta=1} \\ &= \frac{p}{330} - \frac{s}{330} + \frac{329sp}{55} + \frac{1}{55} \end{aligned}$$

$$4. \sigma(I_\alpha(s, p)) = (D_\eta - D_\zeta)^2(\mathbb{M}(I_\alpha(s, p)); \eta, \zeta)$$

$$\begin{aligned} (D_\eta - D_\zeta)^2(\mathbb{F}(\eta, \zeta)) &= 2\eta^5 \zeta^6 (s - p + 6sp - 6) \Big|_{\eta=\zeta=1} \\ &= 2s - 2p + 12sp - 12 \end{aligned}$$

Properties prediction of boron crystal sheet

By emphasizing topological descriptors' importance in QSAR/QSPR research and illustrating their predictive and assessment factors for boron sheets, a key focus of this study is described in this section. Using regression analysis, an equation has been formulated to relate the topological descriptors and the significant properties of boron sheets. With the aid of these formulations, one may further predict the characteristics of boron sheets, independent of their dimensions.

Significance of molecular descriptors

In quantitative structure-activity relationship (QSAR) and quantitative structure-property relationship (QSPR), the topological descriptors, 'describes' the molecular structure's properties or activities in mathematical terminologies. QSAR/QSPR mathematically correlates the physicochemical properties or biological activity of chemical compounds with molecular descriptors. The base for this idea, QSAR/QSPR modelling is many chemical compounds have been implicitly equated with the overall risks which cause acute effects on human health. Some of the pesticide compounds are highly toxic and few may cause cancer.

The toxicological testing of an active ingredient is usually limited. To estimate and rank the potentially hazardous chemicals, it is essential to develop an accurate and simple method³³. Thus, it is a critical need to analyze and understand the structural properties of molecular compounds. Linear regression, multiple linear regression, logistic regression³⁴, efficient linear method³⁵, principal component analysis³⁶, partial least square regression³⁷, decision tree³⁸ and random forest³⁹ are the modelling techniques or methods that are used to analyze or predict the molecular compounds. In our study, linear regression method is deployed for statistical analysis of boron α -icosahedral nanosheet. The graphical flowchart insisting on the topological descriptors and their potential uses is exhibited in Fig. 8.

Variant of boron sheets and its descriptors

Boron has recently received a lot of attention due to its diverse chemical properties and similarities to carbon. Due to the large number of allotropes and complex bonding nature of boron, many are interested to study its crystal structures and stability⁴⁰. Icosahedra exhibit electrical and structural stability as well as interesting chemical

Prediction of the properties of α Icosahedral nanosheet by bond-additive M-polynomial

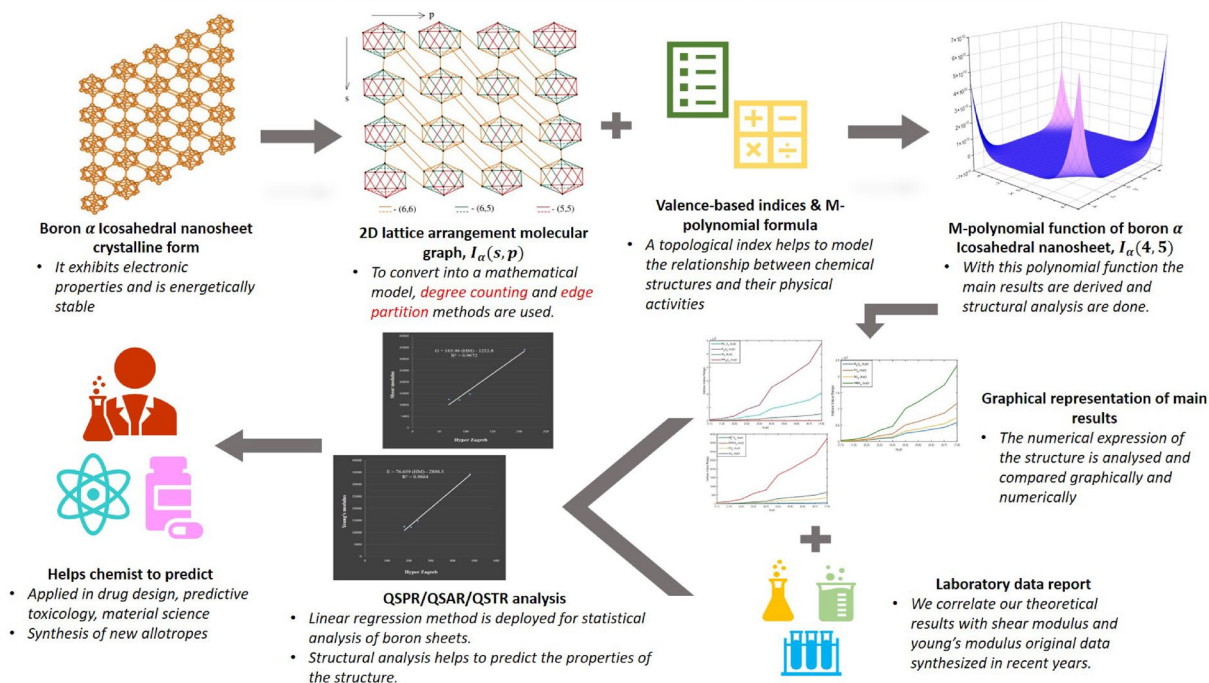


Figure 8. Graphical flowchart indicating the topological descriptors significance.

SI. no	Boron nanosheets	Shear modulus, G	Young's modulus, E
1	α -icosahedral, α - B_{12}	210 GPa	480 N/m
2	α borophene	88 GPa	210 N/m
3	8 - $Pmmn$ borophene	108 GPa	241 N/m
4	β_{12} -borophene	68.5 GPa	179 N/m

Table 5. Experimental data for Young's modulus and shear modulus of boron nanosheets.

bonding characteristics. A few of the two-dimensional boron sheets such as boron α -icosahedral nanosheet, α - B_{12} , α borophene nanosheet⁴¹, 8 - $Pmmn$ borophene nanosheet⁴², β_{12} -borophene nanosheet⁴³ were analyzed through regression analysis. The above-mentioned boron sheet is illustrated in Fig. 9. The degree-vertex value of the base structure of boron sheets is listed in Table 5.

In our study, we investigate the elastic, geometric, thermodynamic, and mechanical properties of the boron sheets. An elastic constant is used to determine the mechanical properties of a material and describe its ability to resist deformation by external forces. With elastic constant, some mechanical properties such as Young's modulus E , bulk modulus B and Shear modulus G can be determined. The elastic properties are closely related to the thermodynamic properties like melting point, heat capacity, vacancy defect, and temperature. The Young's modulus, E , and Shear modulus, G data of various boron nanosheets are summarized in Table 6^{44–46}. The Young's modulus (N/m) indicates a material's ability to withstand changes in length when brought under tension or compression and shear modulus (GPa) is a measure of elastic shear material's stiffness that reflects body rigidity.

Properties analysis and theoretical prediction

The mechanical properties, Young's modulus and shear modulus of the above-mentioned boron sheets are analyzed with topological descriptors by a regression model. Legendre⁴⁷ and Gauss⁴⁸ introduced the least squares approach to linear regression in 1805 and 1809 respectively. Regression analysis is a statistical technique that determines the correlation between two or more variables. The correlation coefficient ranges from 1 to -1. The perfect positive and negative correlation is 1 and -1 where near 0 indicates weak correlation. A correlation coefficient and regression analysis are used to derive the equation connecting the descriptors and properties. The linear regression model,

$$M = i + j(TD)$$

where M is the mechanical properties of the boron nanosheets, and TD is topological descriptors. Using SPSS software^{49,50}, the invariant, i and regression coefficient, j can be calculated. The correlation coefficients between

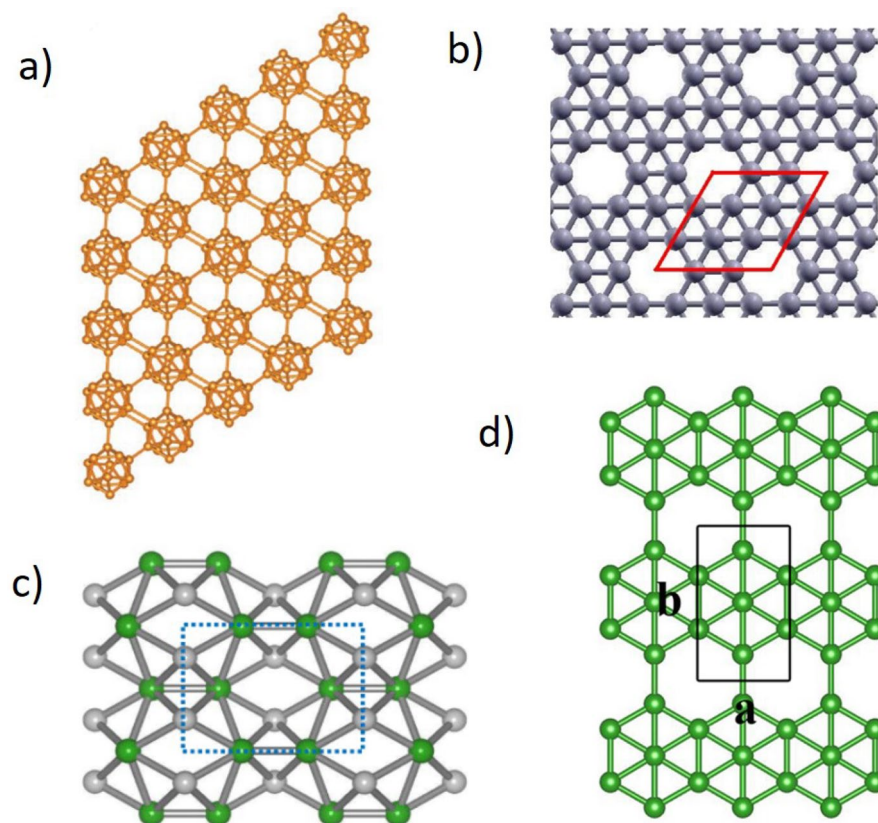


Figure 9. Boron nanosheet and its allotropes; (a) α -icosahedral, α -B₁₂ (b) α borophene (c) 8 - $Pmmn$ borophene (d) β_{12} -borophene.

Indices	α -icosahedral	α -borophene	8 - $pmmn$	β_{12} -borophene
M_1	3140	1222	1364	1318
M_2	8522	2968	3441	3023
M_2^m	10.08	6.1511	6.0986	7.6156
A	10637.932	3520.5917	3910.979	3508.5186
R	8522	2968	3441	3028
RR	10.08	6.1511	6.0986	7.6156
H	53.8545	26.849	26.1612	31.9423
HM	34184	12148	14714	12452
F	17140	6212	7832	6814
σ	96	276	950	360
SDD	583.2	266.667	313.9048	304.9333
I	782.8182	297.9432	316.349	319.6294

Table 6. Degree-vertex value of boron nanosheets.

dependent variables, physical properties of boron sheets and independent variables, topological descriptors of nanosheets are listed in Table 7. For recent work on QSPR analysis by linear regression method, readers can refer^{51,52}.

The correlation table indicates that these boron derivatives have strong correlations within themselves for both chemical attributes. In comparison to other indices, the hyper Zagreb index has a strong correlation for Young's modulus and shear modulus. The linear regression model for shear modulus is shown below,

$$G = 165.46(HM) - 1252.8$$

where G is shear modulus and HM is hyper Zagreb index. Similarly, the linear regression equation for Young's modulus is determined as follows

Indices	Shear modulus, G	Young's modulus, E
M_1	0.9701	0.981
M_2	0.98	0.9915
M_2^m	0.8109	0.8494
A	0.9774	0.9901
R	0.9798	0.9914
RR	0.8109	0.8494
H	0.9013	0.93005
HM	0.9835	0.9932
F	0.9794	0.989
σ	0.39799	0.45497
SDD	0.9636	0.9777
I	0.9645	0.98102

Table 7. Correlation coefficient between properties and descriptors.

$$E = 76.659(HM) - 2898.5$$

where E is Young's modulus. The molecular characteristics with a greater dimension can be predicted with an appropriate regression model. In Fig. 10, the scatter plots for the highest correlated properties and descriptors are shown.

Conclusion

Using a degree-vertex M -polynomial graph technique, the topological indices of the boron α -icosahedral nanosheet are determined. The structural characterization is used to analyse the topological connectivity properties of boron α -icosahedral nanosheet, by combining quantum chemical descriptors with nanosheet results. This research could provide a crucial tool for determining the significance of nanosheets in many areas, such as material science, drug discovery, and predictive toxicology. Furthermore, the topological indices are used in the study of boron α -icosahedral nanosheets and provide QSAR expressions that predict several molecular properties such as band gap, optical and electronic stability, molecular density, enthalpies, conductivity, and so on. In this research, we correlate our theoretical results with the shear modulus and Young's modulus original data synthesized in recent years, which showed a high correlation of 0.9835 and 0.9932 with hyper Zagreb. This type of research has not been explored earlier. So, it has a significant contribution to research by finding a correlation between topological indices and properties of boron allotropes. This allows us to explore other nanosheets, it is left as an open problem for future research.

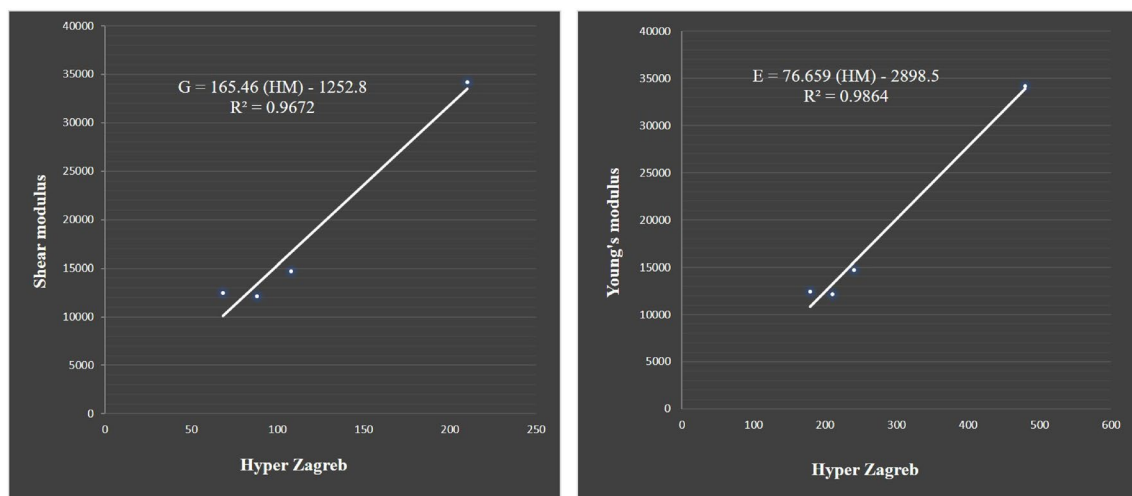


Figure 10. Scatter visualisation for the properties and indices.

Data availability

The datasets generated and/or analyzed during the current study are available in this current article.

Received: 10 August 2023; Accepted: 8 January 2024

Published online: 12 January 2024

References

- Özdoğan, C. *et al.* The unusually stable B₁₀₀ fullerene, structural transitions in boron nanostructures, and a comparative study of alpha- and gamma-boron and sheets. *J. Phys. Chem. C* **114**(10), 4362–4375 (2010).
- Sun, X. *et al.* Two-dimensional boron crystals: Structural stability, tunable properties, fabrications and applications. *Adv. Func. Mater.* **27**(19), 1603300 (2017).
- Li, D., Young-Nian, X. & Ching, W. Y. Electronic structures, total energies, and optical properties of α -rhombohedral b 12 and α -tetragonal b 50 crystals. *Phys. Rev. B* **45**(11), 5895 (1992).
- Wang, L., Mo, Y., Rulis, P. & Ching, W. Y. Spectroscopic properties of crystalline elemental boron and the implications on B 11 C-CBC. *RSC Adv.* **3**(47), 25374–25387 (2013).
- Awasthi, A. & Subhash, G. Deformation behavior and amorphization in icosahedral boron-rich ceramics. *Prog. Mater. Sci.* **112**, 100664 (2020).
- Li, X.-B., Xie, S.-Y., Zheng, H., Tian, W. Q. & Sun, H.-B. Boron based two-dimensional crystals: Theoretical design, realization proposal and applications. *Nanoscale* **7**(45), 18863–18871 (2015).
- Lau, K. C. & Pandey, R. Stability and electronic properties of atomistically-engineered 2D boron sheets. *J. Phys. Chem. C* **111**(7), 2906–2912 (2007).
- HIGASHI, I. & ISHII, T. Two-dimensional icosahedral $b_{<12>}$ networks in boron-rich crystals. *Forma* **16**(3), 187–207 (2001).
- Vickers, N. J. Animal communication: When i'm calling you, will you answer too?. *Curr. Biol.* **27**(14), R713–R715 (2017).
- Albert, B. & Hillebrecht, H. Boron: Elementary challenge for experimenters and theoreticians. *Angew. Chem. Int. Ed.* **48**(46), 8640–8668 (2009).
- Parakhonskiy, G. *Synthesis and Investigation of Boron Phases at High Pressures and Temperatures*. in PhD thesis (2012).
- Cai, Z.-Q., Rauf, A., Ishtiaq, M. & Siddiqui, M. K. On Ve-degree and Ev-degree based topological properties of silicon carbide Si₂C₃-II [p, q]. *Polycyclic Aromat. Compd.* **42**(2), 593–607 (2022).
- Zhang, J., Siddiqui, M. K., Rauf, A. & Ishtiaq, M. On Ve-degree and Ev-degree based topological properties of single walled titanium dioxide nanotube. *J. Cluster Sci.* **32**, 821–832 (2021).
- Deutsch, E. & Klavžar, S. M-polynomial and degree-based topological indices. *arXiv preprint arXiv:1407.1592*, (2014)
- Julietraja, K. & Venugopal, P. Computation of degree-based topological descriptors using M-polynomial for coronoid systems. *Polycyclic Aromat. Compd.* **42**(4), 1770–1793 (2022).
- Julietraja, K., Venugopal, P., Prabhu, S. & Liu, J.-B. M-polynomial and degree-based molecular descriptors of certain classes of benzenoid systems. *Polycyclic Aromat. Compd.* **42**(6), 3450–3477 (2022).
- Shanmukha, M. C., Usha, A., Basavarajappa, N. S. & Shilpa, K. C. M-polynomials and topological indices of styrene-butadiene rubber (SBR). *Polycyclic Aromat. Compd.* **42**(5), 2723–2737 (2022).
- Shanmukha, M. C., Usha, A., Basavarajappa, N. S. & Shilpa, K. C. Comparative study of multilayered graphene using numerical descriptors through m-polynomial. *Phys. Scr.* **98**(7), 075205 (2023).
- Gutman, I. & Trinajstić, N. Graph theory and molecular orbitals. total ϕ -electron energy of alternant hydrocarbons. *Chem. Phys. Lett.* **17**(4), 535–538 (1972).
- Gutman, I., Ruščić, B., Trinajstić, N. & Wilcox, C. F. Jr. Graph theory and molecular orbitals. xII. Acyclic polyenes. *J. Chem. Phys.* **62**(9), 3399–3405 (1975).
- Furtula, B., Graovac, A. & Vukičević, D. Augmented zagreb index. *J. Math. Chem.* **48**, 370–380 (2010).
- Shirdel, G. H., Rezapour, H. & Sayadi, A. M. The hyper-zagreb index of graph operations. (2013).
- Hao, J. Theorems about zagreb indices and modified zagreb indices. *MATCH Commun. Math. Comput. Chem* **65**, 659–670 (2011).
- Randic, M. Characterization of molecular branching. *J. Am. Chem. Soc.* **97**(23), 6609–6615 (1975).
- Bollobás, B. & Erdős, P. Graphs of extremal weights. *Ars Combin.* **50**, 225 (1998).
- Gutman, I., Furtula, B. & Elphick, C. Three new/old vertex-degree-based topological indices. *MATCH Commun. Math. Comput. Chem* **72**(3), 617–632 (2014).
- Zhong, L. The harmonic index for graphs. *Appl. Math. Lett.* **25**(3), 561–566 (2012).
- Favaron, O., Mahéo, M. & Saclé, J.-F. Some eigenvalue properties in graphs (conjectures of graffiti-ii). *Discret. Math.* **111**(1–3), 197–220 (1993).
- Kier, L. B. & Hall, L. H., *et al.* *Molecular connectivity in structure-activity analysis*. Res. Stud., (1986).
- Gupta, C. K., Lokesh, V., Shwetha, S. B. & Ranjini, P. S. On the symmetric division deg index of graph. *Southeast Asian Bull. Math.* **40**(1), 1–23 (2016).
- Furtula, B. & Gutman, I. A forgotten topological index. *J. Math. Chem.* **53**(4), 1184–1190 (2015).
- Sedlar, J., Stevanović, D. & Vasilyev, A. On the inverse sum indeg index. *Discret. Appl. Math.* **184**, 202–212 (2015).
- Sabljić, A. Quantitative structure-toxicity relationship of chlorinated compounds: A molecular connectivity investigation. *Bull. Environ. Contam. Toxicol.* **30**, 80–83 (1983).
- Hosmer, D. W. Jr., Lemeshow, S. & Sturdivant, R. X. *Applied Logistic Regression* Vol. 398 (Wiley, 2013).
- Worachartcheewan, A. *et al.* Predicting metabolic syndrome using the random forest method. *Sci. World J.* **2015**, 581501 (2015).
- Jolliffe, I. T. *Principal Component Analysis for Special Types of Data* (Springer, 2002).
- Helland, I. S. On the structure of partial least squares regression. *Commun. Stat.-Simul. Comput.* **17**(2), 581–607 (1988).
- Salzberg, S. L. C4.5: Programs for Machine Learning by J. Ross quinlan. Morgan Kaufmann Publishers, inc., 1993, (1994).
- Breiman, L. Statistical modeling: The two cultures (with comments and a rejoinder by the author). *Stat. Sci.* **16**(3), 199–231 (2001).
- Oganov, A. R. *et al.* Ionic high-pressure form of elemental boron. *Nature* **457**(7231), 863–867 (2009).
- Meitong, O. *et al.* The emergence and evolution of borophene. *Adv. Sci.* **8**(12), 2001801 (2021).
- Zhang, S.-H., Shao, D.-F. & Yang, W. Velocity-determined anisotropic behaviors of RKKY interaction in 8-Pmmn borophene. *J. Magn. Magn. Mater.* **491**, 165631 (2019).
- Luo, Z., Fan, X. & An, Y. First-principles study on the stability and STM image of borophene. *Nanoscale Res. Lett.* **12**, 1–8 (2017).
- Saha, S., Von Der Linden, W. & Boeri, L. Fused borophenes: A new family of superhard light-weight materials. *Phys. Rev. Mater.* **5**(8), L080601 (2021).
- Wang, Z.-Q., Lü, T.-Y., Wang, H.-Q., Feng, Y. P. & Zheng, J.-C. Review of borophene and its potential applications. *Front. Phys.* **14**, 1–20 (2019).
- Yuan, J., Niannian, Yu., Xue, K. & Miao, X. Ideal strength and elastic instability in single-layer 8-Pmmn borophene. *RSC Adv.* **7**(14), 8654–8660 (2017).
- Legendre, A. M. *Mémoire sur les opérations trigonométriques: dont les résultats dépendent de la figure de la terre*. (No. 1). F. Didot, (1805).

48. Gauss, C. F. *Theoria motus corporum coelestium* (Werke, 1809).
49. Hosamani, S., Perigidad, D., Jamagoud, S., Maled, Y. & Gavade, S. QSPR analysis of certain degree based topological indices. *J. Stat. Appl. Probab.* **6**(2), 361–371 (2017).
50. Consonni, V. & Todeschini, R. *Molecular Descriptors for Chemoinformatics: Volume I: Alphabetical Listing/Volume II: Appendices, References* (Wiley, 2009).
51. Hui, Z. H., Naeem, M., Rauf, A. & Aslam, A. Estimating the physicochemical properties of antiemetics using degree-based topological descriptors. *Mol. Phys.* **121**, e2189491 (2023).
52. Mondal, S., Dey, A., De, N. & Pal, A. QSPR analysis of some novel neighbourhood degree-based topological descriptors. *Complex Intell. Syst.* **7**, 977–996 (2021).

Author contributions

Conceptualization, A.A.; Methodology, A.S.; Software, A.S.; Formal analysis, K.J.; Investigation, K.J., and A.A.; Resources, A.A.; Writing—original draft, A.A. and K.J., A.S.; Supervision, A.A. and D.A.X.

Funding

This work is not funded by government or any private agency.

Competing interests

The authors declare no competing interests.

Additional information

Correspondence and requests for materials should be addressed to A.A.

Reprints and permissions information is available at www.nature.com/reprints.

Publisher's note Springer Nature remains neutral with regard to jurisdictional claims in published maps and institutional affiliations.



Open Access This article is licensed under a Creative Commons Attribution 4.0 International License, which permits use, sharing, adaptation, distribution and reproduction in any medium or format, as long as you give appropriate credit to the original author(s) and the source, provide a link to the Creative Commons licence, and indicate if changes were made. The images or other third party material in this article are included in the article's Creative Commons licence, unless indicated otherwise in a credit line to the material. If material is not included in the article's Creative Commons licence and your intended use is not permitted by statutory regulation or exceeds the permitted use, you will need to obtain permission directly from the copyright holder. To view a copy of this licence, visit <http://creativecommons.org/licenses/by/4.0/>.

© The Author(s) 2024